ESOMAT 2009, 04008 (2009)
DOI:10.1051/esomat/200904008

Rearrangement of crystallographic domains driven by magnetic field in Fe_3Pt and CoO and new phase appearance in Ni_2MnGa

T. Kakeshita[a], T. Terai, M. Yamamoto and T. Fukuda

Department of Materials Science and Engineering, Graduate School of Engineering, Osaka University, 2-1 Yamada-Oka, Suita, Osaka 565-0871, Japan

Abstract. We have investigated the rearrangement of crystallographic domains driven by magnetic field in a ferromagnetic shape memory alloy of Fe_3Pt and an antiferromagnetic oxide of CoO. Also, we have determined the equilibrium stress-temperature phase diagram in a ferromagnetic shape memory alloy of Ni_2MnGa. Following result are obtained ; (i) We confirm that magnetic field promotes the rearrangement of crystallographic domains in Fe_3Pt and CoO and the condition of the rearrangement in the present two systems is the same, that is, the magnetic shear stress, which corresponds to the magnetic anisotropy energy divided by the twinning shear, is equal to or larger than the twinning stress. (ii) We construct the equilibrium stress-temperature phase diagram of Ni_2MnGa by compressive tests and magnetic susceptibility measurements, and show the existence of the new phase of X-phase. Moreover, we evaluate the triple point at which the I-, P- and X-phases coexist and suggest the existence of a critical point of the successive P → X → I transformation.

1. Introduction

Recently, it has been found that a large magnetic field-induced strain (MFIS) of several percent appears in some ferromagnetic shape memory alloys by applying magnetic field [1-3]. This phenomenon is of interest because magnetic field influences not only its intensive variable but also another variable of strain. This large MFIS in ferromagnetic shape memory alloys is not due to the conventional magnetostriction, but due to the rearrangement of crystallographic domains (variants) of the martensite under a magnetic field. We discussed about this energy evaluation and derived the condition for the occurrence of the rearrangement driven by magnetic field. That is, we introduce a shear stress acting across a twinning plane driven by magnetic field (We call it a magnetic shear stress), τ_{mag}, considering the fact that the twinning plane movement certainly occurs by magnetic field [4]. The value of τ_{mag} is expressed as,

$$\tau_{mag} = \frac{\Delta U_{mag}}{s}, \qquad (1)$$

where ΔU_{mag} is the magnetic energy difference per unit volume between the two crystallographic domains separated by the twinning plane, and s is the corresponding twinning shear. Using this value, the condition for the occurrence of the rearrangement of crystallographic domains is derived: the value of τ_{mag} is equal to or larger than the shear stress required for the twinning plane movement, τ_{req}. This condition was confirmed to be appropriate for ferromagnetic shape memory alloys of Ni_2MnGa and Fe–31.2Pd (at.%) [4,5].

In the previous paper [6], we found that Fe_3Pt shows the MFIS below the martensitic transformation temperature, T_M =85 K, and the behavior of MFIS was different from that of Ni_2MnGa and Fe–31.2Pd. That is, the fraction of the most preferable crystallographic domain, which has the lowest magnetic energy, does not reach 100% under a magnetic field applied along $[0\ 0\ 1]_P$ direction, and a part of the MFIS recovers in the field removing process. However, it has not been confirmed whether the rearrangement condition mentioned above is appropriate for Fe_3Pt or not. Furthermore, this condition implies that whenever the τ_{mag} is equal to or larger than τ_{req}, all the materials having crystallographic domains can come to exhibit the rearrangement irrespective of their magnetism. However, the validity of this condition has not been confirmed in the materials other than ferromagnetic shape memory alloys. To solve these problems is one of the purpose of the present study. The other is described below.

The stoichiometric Ni_2MnGa transforms from an $L2_1$-type parent phase (P-phase) to an intermediate phase (I-

[a] e-mail : kakesita@mat.eng.osaka-u.ac.jp

phase) at about 250 K, then further transforms to a martensite phase (M-phase) at about 200 K on cooling [7-9]. In addition to these phases, we recently found that a new phase, the X-phase, is induced from the P- and I phases by applying a compressive stress in the $[001]_P$ (p represents the P-phase) direction [10]. Karaman *et al*. [11] reported that the reversible MFIS can be realized by using the magnetic field-induced X ↔ I transformation. Thus, the X-phase is important from both the fundamental point of view and from an applied point of view such as actuators. In our previous study [10], we constructed a phase diagram by using the transformation start stress and transformation start temperature. However, these values are not equilibrium ones, and we need the equilibrium phase diagram if we undertake a thermodynamic analysis.

In this paper, we will investigate in detail the rearrangement of crystallographic domain driven by magnetic field in an iron-based ferromagnetic shape memory alloy of Fe_3Pt and an antiferromagnetic oxide of CoO and show that the validity of the condition mentioned above for the rearrangement of crystallographic domains in Fe_3Pt and CoO. Furthermore, we will construct the equilibrium stress-temperature phase diagram determined by compressive tests and magnetic susceptibility measurements in Ni_2MnGa.

2. Experimental Procedure

Single crystals of Fe_3Pt, CoO and Ni_2MnGa were prepared by a floating zone method. The degree of order of Fe_3Pt is about 0.8, which was confirmed by an X-ray diffraction. The grown crystals were cut into a parallelepiped for optical microscope observations and magnetostriction measurements after determining the orientation by a Laue camera. The temperature dependence of MFIS of Fe_3Pt was measured by strain gauge method. The change in morphology of the surface in CoO under a magnetic field was observed by inclining the incident beam in an optical microscopy. The magnetization of the specimens of Fe_3Pt, CoO and Ni_2MnGa was measured by a SQUID magnetometer, and the compressive tests of CoO and Ni_2MnGa were performed by an Instron-type testing machine.

3. Results and Discussion

3.1 Rearrangement of crystallographic domains in ferromagnetic shape memory alloy of Fe_3Pt

We have investigated the rearrangement of crystallographic domains for Fe_3Pt under the magnetic field of $[1\ 1\ 1]_P$, $[1\ 1\ 0]_P$ and $[1\ 1\ 1]_P$ (p represents parent phase) directions. The result obtained under magnetic field up to 3.2 MA/m at 4.2 K is shown in Fig. 1. As known from the figure, the single crystal contracts under the $[0\ 0\ 1]_P$ field and expands under the $[1\ 1\ 0]_P$ field. This means that the preferable crystallographic domain under the magnetic field is selected, where, the preferable crystallographic domains is the one whose *c*-axis (easy axis) lies along the field direction under the $[0\ 0\ 1]_P$ field and the ones whose *c*-axis forms an angle of about 45° with the field direction under the $[1\ 1\ 0]_P$ field. Concerning the $[1\ 1\ 1]_P$ field, no specific domain is selected by the field application, meaning that rearrangement of domains does not occur by magnetic field.

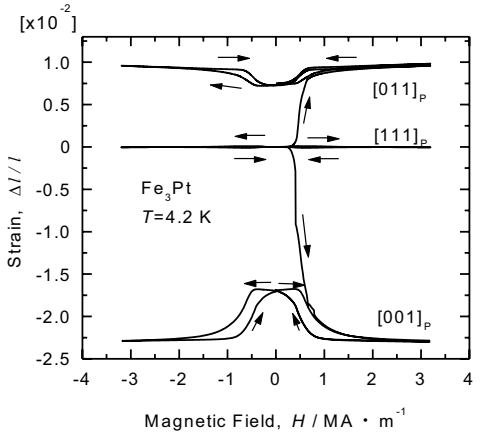

Fig. 1 Magnetic field-induced strain of an Fe_3Pt single crystal measured at 4.2 K under the $[001]_P$, the $[011]_P$ and the $[111]_P$ fields.

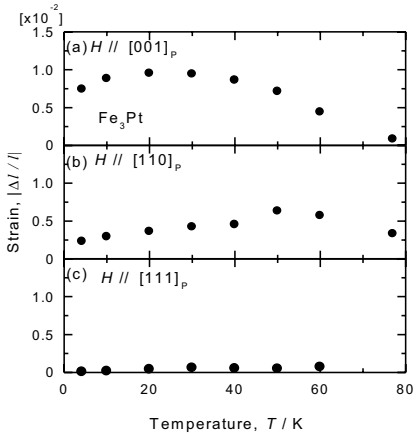

Fig. 2. Temperature dependence of the recoverable strain of an Fe_3Pt single crystal under the magnetic field at 3.2MA/m applied along (a) $[001]_P$, (b) $[011]_P$ and (c) $[111]_P$.

In order to confirm the validity of the condition, $\tau_{mag} \geq \tau_{req}$, in Fe_3Pt, we have to evaluated the value of $\tau_{mag} = \Delta U_{mag}/s$. In the previous study [4], the maximum values of ΔU_{mag} are obtained as the magnetocrystalline anisotropy constant, $|K_u|$, under the $[0\ 0\ 1]_P$ field, $|K_u|/2$ under the $[1\ 1\ 0]_P$ field and zero under the $[1\ 1\ 1]_P$ field,

respectively. From the magnetization measurements, we obtain the value of $|K_u|$ and it is about 4×10^2 kJ / m^3. Then, we obtained the value of s by using the reported lattice parameters [12] and it is 0.12. By using these values, the obtained maximum values of τ_{mag} are about 4 MPa under the $[0\ 0\ 1]_P$ field, about 2 MPa under the $[1\ 1\ 0]_P$ field and 0 MPa under the $[1\ 1\ 1]_P$ field, respectively. The other important quantity is τ_{req} and it was obtained by compressive tests along the $[0\ 0\ 1]_P$ direction. The obtained value is about 1 MPa. From these values, we confirm when the τ_{mag} is equal to or larger than τ_{req}, the rearrangement of crystallographic domains occurs.

Incidentally, the temperature dependence of the reversible MFIS is shown in Fig. 2. As known from the figure, the reversible MFIS under the $[0\ 0\ 1]_P$ and $[1\ 1\ 0]_P$ fields depend on temperature and the maximum value reaches about 1 % at 20 K under the $[0\ 0\ 1]_P$ field. The reason for the occurrence of the reversible MFIS is not known yet, but may be related to some defects introduced in Fe_3Pt (e.g. degree of order). We also have calculated the electronic structure of Fe_3Pt and found that the electronic structure has a peak in the density of states of the minority spin band just below the Fermi energy. This peak splits into two peaks by tetragonal distortion, and one of them shifts to lower energy by the distortion, suggesting that the band Jahn-Teller effect is the main cause for the transformation.

3.2 Rearrangement of crystallographic domains in antiferromagnetic oxide of CoO

The paramagnetic to antiferromagnetic transition of CoO is associated with a structure change from a cubic structure ($Fm\bar{3}m$) to a pseudo-tetragonal one [13,14]. The magnetic moment is reported to be aligned in the [117] direction, which is nearly parallel to the *c*-axis of the tetragonal phase. Thus the magnetic susceptibility in the *a*-axis should be larger than that in the *c*-axis, therefore, there arises magnetic energy difference between crystallographic domains under a magnetic field. In the following, we will show that this magnetic energy difference causes rearrangement of crystallographic domains in antiferromagnetic CoO, as in the ferromagnetic Fe_3Pt alloy.

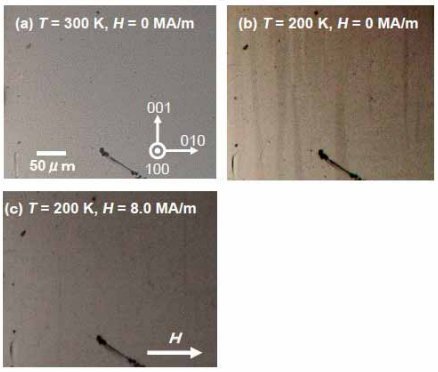

Fig. 3 A series of optical micrograph showing the rearrangement of crystallographic domainss under magnetic field

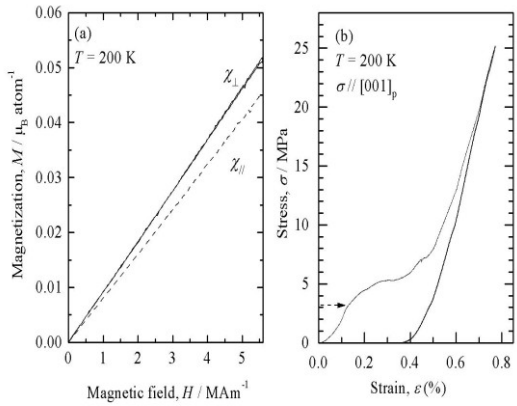

Fig.4. Magnetization and Stress-Strain curves of CoO at 200 K.

Figure 3(a) shows the plane microstructure of paramagnetic cubic phase at 300 K. When the temperature of the specimen is lowered below the Néel temperature of 293 K, a twinned microstructure appears as shown in Fig. 3(b). Then, we apply a magnetic field in the $[001]_P$ direction of the twinned specimen at 200 K. When the magnetic field of 8.0 MA/m is applied, the dark region changes to the bright region as shown in Fig. 3(c). This result shows the occurrence of the rearrangement of crystallographic domains, and a large strain of about 1 % appears in association with the rearrangement.

In order to confirm whether or not the condition for the rearrangement of crystallographic domains by magnetic field described in ferromagnetic Fe_3Pt is satisfied for the present antiferromagnetic CoO, we have evaluated τ_{mag} and τ_{req}. The magnetic energy difference between the domains, ΔU_{mag}, is given as,

$$\Delta U_{mag} = \frac{(\chi_{\perp} - \chi_{//})H_0^2}{2}, \qquad (2)$$

where H_0 is the applied magnetic field, and $\chi_{//}$ and $\chi_{\perp}$ are the magnetic susceptibility obtained for the direction which is parallel and perpendicular to magnetic moment of Co^{2+} ion, respectively. In order to obtain the value of ΔU_{mag}, we measure magnetization curves along $\langle 100 \rangle_t$ and $\langle 001 \rangle_t$ (t represents the tetragonal phase and $\langle 001 \rangle_t$ is the *c*-axis) directions in a single domain state of the tetragonal phase, which is obtained by loading a compressive stress along a $\langle 001 \rangle_p$ (p represents the parent phase) direction. The result is shown in Fig. 4(a). The value of ΔU_{mag} obtained by these magnetization curves is 28.0 kJ/m^3 at 8.0 MA/m. The twinning shear s is calculated to be 1.14×10^{-3} from the lattice parameter obtained by an X-ray experiment. Then τ_{mag} at 200K under

8.0 MA/m is calculated by using the equation of $\Delta U_{mag}/s$ and its value is 2.53 MPa. The value of τ_{req} has been obtained by a compressive test. Figure 4(b) shows the stress-strain curve applying compressive stress along $\langle 001 \rangle_p$ direction at 200 K. As known from the figure, we notice a stage due to the rearrangement of crystallographic domains. The value of τ_{req} is obtained by multiplying the Schmid factor to the stress of this stage and the obtained value is 1.50 MPa. We know from these results that the condition $\tau_{mag} \geq \tau_{req}$ is obviously satisfied even in an antiferromagneic CoO, as in ferromagnetic Fe_3Pt alloy, when the rearrangement of crystallographic domainss occurs under magnetic field.

3.3 Equilibrium stress-temperature phase diagram of Ni_2MnGa

Figure 5 shows the equilibrium stress-temperature phase diagram of Ni_2MnGa determined by the present study. The symbols P, I, X and M stand for the corresponding phases. In the following, we show how the phase boundaries in Fig. 5 are determined.

First of all, we show the equilibrium stress between the P- and X-phases. For the compressive test, we use a strain gage that is sensitive to small changes in strain. A typical stress–strain curve obtained at 260 K is shown in Fig. 6(a), where the initial state is the P-phase. The curve has an obvious bend point due to the P → X transformation, indicated by the arrow. Since there is no hysteresis between the mechanical loading and unloading processes, the stress $\sigma_{0,P\leftrightarrow X}$ indicated by the arrow corresponds to the equilibrium stress between the P- and X-phases. The absence of the hysteresis suggests that P ↔ X is possibly a second-order transformation. The values of $\sigma_{0,P\leftrightarrow X}$ thus obtained in the temperature range of 258 K ≤ T ≤ 266 K are shown in Fig. 5 by solid circles. Below 258 K, the equilibrium stress $\sigma_{0,P\leftrightarrow X}$ cannot be detected even by attaching the strain gage because the bend point on the stress–strain curve is obscure in the small stress region. Therefore, we determine the phase boundary of the P ↔ X transformation in this region by magnetic susceptibility measurements, which are described later.

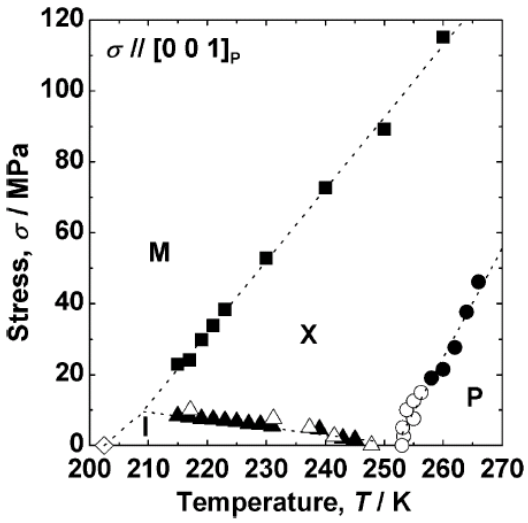

Fig. 5 Stress-temperature equilibrium phase diagram of stoichiometric Ni_2MnGa under a compressive stress applied in the $[001]_P$ direction.

The X-phase induced from the P-phase described above transforms to the M-phase by further increasing the compressive stress. That is, a successive P → X → M transformation occurs. Since the strain gage peels off during the X → M transformation, we measure the stress–strain curves instead by calibrating the movement of the cross-head. A typical stress–strain curve obtained at 260 K is shown in Fig. 6(b), where the initial state is the P-phase. In the curve, the bend point due to the P → X transformation described above is not clear, only the stage due to the X → M transformation appearing clearly. This stage starts at $\sigma_{s,X\rightarrow M}$, as indicated by an arrow in the mechanical loading process. The unloading process also has only one stage due to the M → X transformation, and this stage finishes at $\sigma_{f,M\rightarrow X}$ as indicated by a double arrow. We define the equilibrium stress between the X- and M-phases, $\sigma_{0,X\leftrightarrow M}$, as the average of $\sigma_{s,X\rightarrow M}$ and $\sigma_{f,M\rightarrow X}$. Similar measurements have been made at 250 K and the values of $\sigma_{0,X\leftrightarrow M}$ are shown in Fig. 5 by solid squares.

In order to determine the equilibrium stress between the I- and X-phases, we have made a compressive test by attaching a strain gage. A typical stress–strain curve obtained at 219 K is shown in Fig. 6(c), where the initial state is the I-phase. The curve has one stage due to the I → X transformation, starting at $\sigma_{s,I\rightarrow X}$, as indicated by an arrow in the mechanical loading process. In the unloading process, the curve also has one stage due to the X → I transformation, finishing at $\sigma_{f,X\rightarrow I}$, as indicated by a double arrow. Taking the average of $\sigma_{s,I\rightarrow X}$ and $\sigma_{f,X\rightarrow I}$, we de-

fine the equilibrium stress between the I- and X-phases, $\sigma_{0,I\leftrightarrow X}$. The values of $\sigma_{0,I\leftrightarrow X}$ obtained in the temperature range of 215 K ≤ T ≤ 245 K are shown in Fig. 5 by solid triangles.

The X-phase induced from the I-phase described above transforms into the M-phase. That is, a successive I → X → M transformation occurs [9]. Since the strain gage peels off in the high strain region, we have measured the stress–strain curves in stead by calibrating the movement of the cross-head. A typical stress–strain curve at 219 K is shown in Fig. 6(d), where the initial state is the I-phase. The curve has two stages due to the successive I → X → M transformation in the mechanical loading process. That is, the first stage, starting at $\sigma_{s,I\rightarrow X}$ is due to the I → X transformation and the second one, starting at $\sigma_{s,X\rightarrow M}$, is due to the X → M transformation. The curve also has two stages in the unloading process. The first stage, finishing at $\sigma_{f,M\rightarrow X}$ is due to the M → X transformation and the second one, finishing at $\sigma_{f,X\rightarrow I}$ is due to the X → I transformation. The values of $\sigma_{s,I\rightarrow X}$ and $\sigma_{f,X\rightarrow I}$ agree with those obtained by attaching the strain gage, mentioned above. We determine the equilibrium stress between the X- and M-phases, $\sigma_{0,X\leftrightarrow M}$, as the average of $\sigma_{s,X\rightarrow M}$ and $\sigma_{f,M\rightarrow X}$, as described above. The values of $\sigma_{0,X\leftrightarrow M}$ obtained in the temperature range of 215 K ≤ T ≤ 240 K are shown in Fig. 5 by solid squares. Bellow 215 K, the reverse transformations (X →I, M → X and M → I transformations) in the unloading process are not complete. Therefore, we cannot determine the equilibrium stresses, $\sigma_{0,I\leftrightarrow X}$, $\sigma_{0,X\leftrightarrow M}$ and $\sigma_{0,I\leftrightarrow M}$, using only compressive tests. The phase boundaries in this region will be determined later by a thermodynamic calculation.

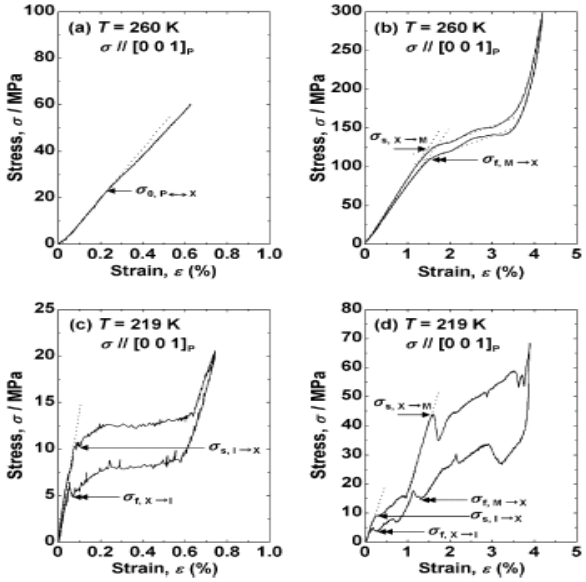

Fig. 6 Stress–strain curves of Ni_2MnGa obtained by applying compressive stress in

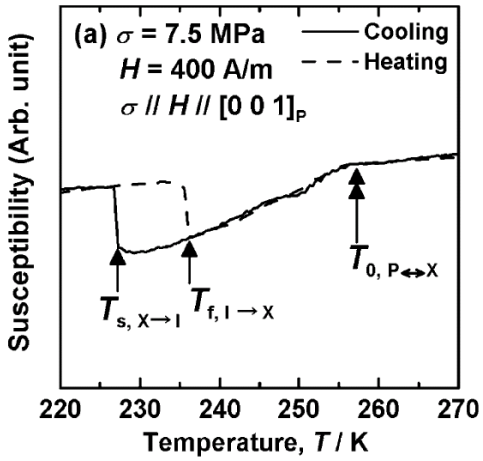

Fig. 7 Magnetic susceptibility of Ni_2MnGa measured under constant compressive stresses of 7.5 MPa applied in the $[001]_P$ direction.

In order to determine the phase boundary of the P ↔ X transformation below 258 K which cannot be determined by compressive tests, as mentioned above, we took magnetic susceptibility measurements under a constant compressive stress because this is also sensitive to the transformation. Figure 7 shows a typical magnetic susceptibility curve, which was obtained under a compressive stress of 7.5 MPa applied in the $[001]_P$ direction. In the cooling process, the susceptibility starts to decrease at $T_{0,P\leftrightarrow X}$, as indicated by a double arrow, due to the P ↔ X transformation, and then increases abruptly at $T_{s,X\rightarrow I}$, as indicated by an arrow, due to the X → I transformation. In the heating process, the I → X transformation finishes at $T_{f,I\rightarrow X}$ and the X → P transformation occurs at $T_{0,P\leftrightarrow X}$. Since there is no hysteresis in the cooling and heating processes, the temperature, $T_{0,P\leftrightarrow X}$, indicated by the double arrow corresponds to the equilibrium temperature between the P- and X-phases. The absence of the hysteresis suggests again that the P ↔ X transformation is possibly second order. On the other hand, we define the equilibrium temperature between the X- and I-phases, $T_{0,X\leftrightarrow I}$, as the average of $T_{s,X\rightarrow I}$ and $T_{f,I\rightarrow X}$. The values of $T_{0,P\leftrightarrow X}$ and $T_{0,X\leftrightarrow I}$ obtained in the stress range of 0 MPa ≤ σ ≤ 15 MPa are shown in Fig. 5 as open circles and open triangles, respectively. As can be seen from the figure, the phase boundaries of the P ↔ X and I ↔ X transformations obtained by two different methods (stress–strain curve and magnetic susceptibility) are in good agreement each other. This is consistent with the requirement of the equilibrium phase diagram.

In this way, we have determined the phase boundaries of the I ↔ X, P ↔ X and X ↔ M transformations shown in Fig. 5 by the stress–strain curves shown in Fig. 6 and magnetic susceptibility curves shown in Fig. 7. The slopes of these phase boundaries are −0.24 MPa K^{-1} (I ↔ X), 3.08 MPa K^{-1} (P ↔ X) and 2.03 MPa K^{-1} (X ↔ M). The I ↔ M phase boundary still remains to be determined. However, we cannot determine it from compressive tests because the reverse transformation is not complete, as mentioned above. In the following, we

will determine the I ↔ M phase boundary and suggest the existence of a triple point, where the I-, M- and X-phases coexist, based on the thermodynamic requirement.

Since the stress-induced I ↔ M transformation is observed at 203 K ≤ T < 209 K and the extended lines of the I ↔ X and X ↔ M phase boundaries seem to merge at about 209 K, we can say that there should exist a triple point at the intersection of the I ↔ X and X ↔ M phase boundaries. Here we consider the entropy change for an enclosed path surrounding the triple point. Since entropy is a state function, the total entropy change for this enclosed path should be zero. Then the following relation is derived in the vicinity of the triple point:

$$\Delta S_{I\to M} + \Delta S_{M\to X} + \Delta S_{X\to I} = 0. \quad (3)$$

Here, $\Delta S_{A\to B}$ is the entropy change associated with the A → B transformation, which should satisfy the Clausius–Clapeyron equation as,

$$\frac{d\sigma}{dT} = -\frac{\Delta S_{A\to B}}{\Delta \varepsilon_{A\to B}}, \quad (4)$$

where $d\sigma/dT$ is the slope of the phase boundary and $\Delta\varepsilon_{A\to B}$ is the A → B transformation strain. Putting Eq. (3) into Eq. (4), we obtain the following relation,

$$\Delta \varepsilon_{I\to M}\left(\frac{d\sigma}{dT}\right)_{I\to M} = \Delta \varepsilon_{I\to X}\left(\frac{d\sigma}{dT}\right)_{I\to X} + \Delta \varepsilon_{X\to M}\left(\frac{d\sigma}{dT}\right)_{X\to M}. \quad (5)$$

We already know from Fig. 5 that the slope $(d\sigma/dT)_{I\to X}$ is −0.24 MPa K^{-1} and $(d\sigma/dT)_{X\to M}$ is 2.03 MPa K^{-1}. Also, we already know from stress–strain curves at T = 215 and 203 K (these are the nearest temperatures at which transformation strains can be detected) that $\Delta\varepsilon_{I\to X}$ is 0.59%, $\Delta\varepsilon_{X\to M}$ is 2.9% and $\Delta\varepsilon_{I\to M}$ is 3.9%. Putting these values in Eq. (5), the slope $(d\sigma/dT)_{I\to M}$ for the I ↔ M phase boundary is calculated to be 1.47 MPa K^{-1}. The I ↔ M phase boundary with this slope is drawn from the equilibrium temperature in the absence of external stress, $T_{0,I\leftrightarrow M}$, and is shown by a dotted line in Fig. 5. It should be noted that this boundary merges with the I ↔ X and X ↔ M phase boundaries at the same point. This result is consistent with the requirement of the triple point, where the I-, X- and M-phases coexist. The temperature and stress of the triple point are 208.9 K and 9.6 MPa, respectively. Incidentally, the P↔ X phase boundary is almost identical to that of X ↔ I in the absence of external stress, and it suggests the existence of critical point of the successive P → X → I transformation. Kushida *et. al*. performed neutron and synchrotron X-ray diffraction measurements for I-, X- and M-phases [15,16], and found that the X-phase has an incommensurate structure and the positions of the satellite reflection, $[h\ \ h-2\ \ 0]^*_P$, are close to those of I-phase. In future, we will need to identify the difference in the crystal structures of the I-, X- and M-phases.

4. Coclusion

We have investigated the rearrangements of crystallographic domains in Fe_3Pt and CoO. We confirm that the magnetic field promotes the twinning plane movement in a ferromagnetic shape memory alloy of Fe_3Pt and even an antiferromagnetic oxide of CoO. We have found that the condition of the rearrangement defined as $\tau_{mag} \geq \tau_{req}$ is the same in between the present two systems. In addition, we have constructed the equilibrium stress-temperature phase diagram of Ni_2MnGa and shown the existence of the new phase of X-phase. Moreover, we suggest the existence of the triple point at which the I-, P- and X-phases coexist and the critical point of the successive P → X → I transformation.

Acknowledgements

This work is partly supported by Priority Assistance for the Formation of Worldwide Renowned Centers of Research–The Global COE Program (Project: Center of Excellence for Advanced Structural and Functional Materials Design) from MEXT of Japan.

References

[1] K. Ullakko, J. K. Huang, C. Kantner, R. C. O'Handley, V. V. Kokorin, Appl. Phys. Lett. **69**, 1966 (1996).
[2] S. J. Murray, M. A. Marioni, A. M. Kukla, J. Robinson, R. C. O'Handley S. M. Allen, J. Appl. Phys. **87**, 5774 (2000).
[3] T. Sakamoto, T. Fukuda, T. Kakeshita, T. Takeuchi, K. Kishio, J. Appl. Phys. **93,** 8647 (2003).
[4] T. Fukuda, T. Sakamoto, T. Terai, T. Kakeshita, K. Kishio, Matar Res Soc Symposium - Proceedings p 785 (2003).
[5] N. Okamoto, T. Fukuda, T. Kakeshita, Sci. Technol. Adv. Mater. **5**, 29 (2004).
[6] T. Kakeshita, T. Takeuchi, T. Fukuda, M. Tsujiguchi, T. Saburi, R. Oshima, S. Muto, Appl. Phys. Lett. **77**, 1502 (2000).

[7] P.J. Webster, K.R.A. Ziebeck, S.L. Town, M.S. Peak, Philos. Mag. B **49**, 295 (1984).
[8] V.A. Chernenko and V.V. Kokorin, Proceedings of the International Conference on Martensitic Transformation, Monterey Institute of Advanced Studies, edited by C.M. Wayman and J. Perkins, p. 1205 (1992).
[9] A. Planes, E. Obrado´ , A.G. Comas, L. Mano˜ sa, Phys. Rev. Lett. **79**, 3926 (1997).
[10] J.H. Kim, T. Fukuda, T. Kakeshita, Scripta Mater. **54,** 585 (2006).
[11] I. Karaman, H.E. Karaca, B. Basaran, D.C. Lagoudas, Y.I. Chumlyakov, H.J. Maierd, Scripta Mater. **55**, 403 (2006).
[12] T. Sakamoto, T. Fukuda, T. Kakeshita, T. Takeuchi, K. Kishio, Sci. Technol. Adv. Mater. **5**, 35 (2004).
[12] T. Kakeshita, T. Fukuda, T. Takeuchi, Mat. Sci Eng. A **438-440**, 12 (2006).
[13] N. C. Tombs and H. P. Rooksby, Nature **165**, 442 (1950).
[14] S. Greenwald and J. S. Smart, Nature **166**, 523 (1950).
[15] H. Kushida, K. Fukuda, T. Terai, T. Fukuda, T. Kakeshita, T. Ohba, T. Osakabe, K. Kakurai, and K. Kato, Eur. Phys. J. Special Topics **158**, 87 (2008).
[16] H. Kushida, T. Terai,T. Fukuda, T. Kakeshita,T. Osakabeb and K. Kakurai, Scripta Mater. **60** 248 (2009).